Journal of Statistical Physics, Vol. 80, Nos. 5/6, 1995

Phase Separation of Symmetrical Polymer Mixtures in Thin-Film Geometry

Y. Rouault,[1,2] J. Baschnagel,[1,3] and K. Binder[1]

Received December 2, 1994; final April 13, 1995

Monte Carlo simulations of the bond fluctuation model of symmetrical polymer blends confined between two "neutral" repulsive walls are presented for chain length $N_A = N_B = 32$ and a wide range of film thickness D (from $D = 8$ to $D = 48$ in units of the lattice spacing). The critical temperatures $T_c(D)$ of unmixing are located by finite-size scaling methods, and it is shown that $T_c(\infty) - T_c(D) \propto D^{-1/\nu_3}$, where $\nu_3 \approx 0.63$ is the correlation length exponent of the three-dimensional Ising model universality class. Contrary to this result, it is argued that the critical behavior of the films is ruled by two-dimensional exponents, e.g., the coexistence curve (difference in volume fraction of A-rich and A-poor phases) scales as $\phi_{coex}^{(2)} - \phi_{coex}^{(1)} = \hat{B}(D)[1 - T/T_c(D)]^{\beta_2}$, where β_2 is the critical exponent of the two-dimensional Ising universality class ($\beta_2 = 1/8$). Since for large D this asymptotic critical behavior is confined to an extremely narrow vicinity of $T_c(D)$, one observes in practice "effective" exponents which gradually cross over from β_2 to β_3 with increasing film thickness. This anomalous "flattening" of the coexistence curve should be observable experimentally.

KEY WORDS: Monte Carlo simulation; thin films of symmetrical polymer mixtures; phase separation; crossover scaling; critical temperature; phase diagram in the thermodynamic limit.

1. INTRODUCTION AND THEORETICAL BACKGROUND

Thin polymeric films have found increasing scientific interest recently, and also various applications. Considering two-component polymer blends in a thin-film geometry, there is an interesting interplay between the surface effects at the walls and the finite-size effects due to the smallness of the

[1] Institut für Physik, Johannes-Gutenberg Universität, D-55099 Mainz, Germany.
[2] Permanent address: INRA Versailles, Science du Sol, F-78026 Versailles, France.
[3] To whom correspondence should be addressed.

822/80/5-6-6

thin-film thickness D.[1-7] Since in experiments one typically works with two nonequivalent surfaces (e.g., the polymer film covers a solid substrate and is exposed to vacuum or air on the other side), and these surfaces are not "neutral", i.e., one of the two species (A, B) will be preferentially attracted by the surfaces, these experiments are not straightforward to interpret. Note that due to slow kinetics[2-7] it is not always easy to characterize the true equilibrium behavior of such films.

While for other systems [e.g., magnetic thin films[8-10] (see ref. 8, for review), liquid-gas systems[11-14] (see ref. 14 for a brief general review), etc.] the phase transitions in such a confined geometry have been studied theoretically for a long time, the theoretical analysis of the phase separation in thin polymer blend films has only been considered recently .[15-17] This might be due to the fact that already the phase separation in bulk polymer mixtures poses challenging problems. As is well known, the fluctuations of the volume fraction ϕ (of species A in a binary mixture of A and B chains) are correlated over a length scale ξ which diverges as $\xi \propto |1 - T/T_c|^{-\nu}$ as the critical temperature T_c of the phase separation is approached. The strength of this divergence is determined by the critical exponent ν of the correlation length. Mean-field theory (or Ginzburg–Landau theory, respectively) predicts $\nu = \nu_{GL} = 1/2$. However, this mean-field behavior is *not* observed very close to T_c, but only further away, where ξ is smaller than a "crossover length" ξ_{cross} [see Eq. (2)]. Instead, if $\xi > \xi_{cross}$, one expects the bulk (three-dimensional) polymer mixture to exhibit the *same* critical behavior as the three-dimensional Ising model.[18,19] This behavior will be modified significantly in a thin-film geometry, since the thickness of the film D enters as another length scale which affects the values of both the critical temperature and the critical exponents. Several regimes must then be distinguished as shown in Fig. 1. If $\xi \gg D \geqslant \xi_{cross}$, the mixture should essentially behave as a *two-dimensional* system, i.e., one expects $\xi \propto |1 - T/T_c|^{-\nu_2}$, where $\nu_2 = 1$ is the critical exponent of the correlation length of the two-dimensional Ising model, whereas the *three-dimensional* bulk behavior is supposed to be recovered in the limit $D \to \infty$, i.e., for $D \gg \xi > \xi_{cross}$. Thus, there are three types of critical behavior that compete with each other in a thin polymer film: three-dimensional Ising (for $D \gg \xi > \xi_{cross}$), two-dimensional Ising (for $\xi \gg D \geqslant \xi_{cross}$), and mean-field behavior (for $D > \xi_{cross} > \xi$).

The interplay of D and ξ_{cross} during the unmixing phase transition of an AB polymer blend and its influence on the position of the critical temperature in the thin film has been studied recently in the framework of mean-field theory.[15-17] Tang *et al.*[15] adapt the well-known[8,9] Ginzburg–Landau type treatment to polymer films with two equivalent neutral walls (no preferential attraction of a species to a wall). For thick films they find

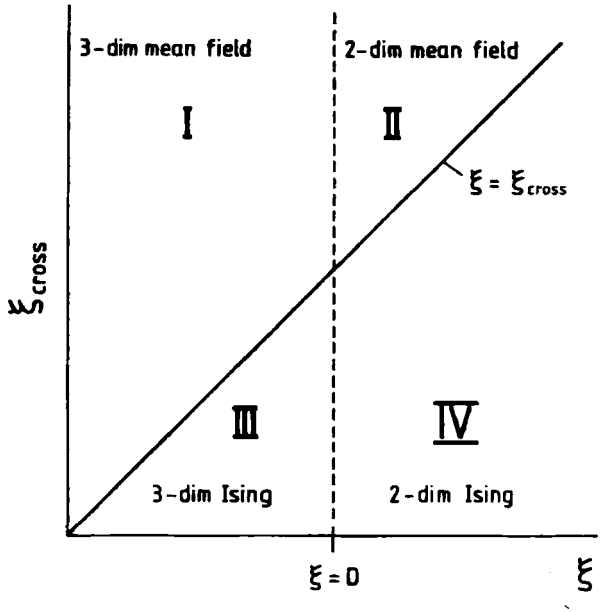

Fig. 1. Schematic description of the regimes where different critical behavior is expected for a polymer mixture. The correlation length ξ can be varied by choosing suitable temperature distances from the critical point, while the crossover correlation length ξ_{cross} can be varied by choosing suitable chain lengths [see Eq. (2)]. A crossover from three-dimensional ($3d$) to two-dimensional ($2d$) critical behavior is expected when $\xi \approx D$, while a crossover from mean-field to Ising behavior is expected when $\xi \approx \xi_{cross}$. In the Ising regime the dimensional crossover ($3d \rightarrow 2d$, from regime III to IV) implies a change of critical exponents, while in the mean-field regime the three-dimensional crossover (from regime I to II) implies only a change of critical amplitude prefactors. Note that the regime very close to the origin is not physically meaningful (both ξ and ξ_{cross} need to exceed the radius of gyration of the chains in order that critical behavior can be observed.)

a shift $T_c(\infty) - T_c(D) \propto D^{-2}$, as expected from a mean field theory, since the general scaling relation for the critical point shift is[8-11, 14, 20]

$$T_c(\infty) - T_c(D) \propto D^{-1/\nu} \tag{1}$$

with $\nu = \nu_{GL} = 1/2$, as mentioned above. For film thickness D less than the crossover length[18, 21, 22], [4]

$$\xi_{cross} \propto bN \tag{2}$$

[4] For conditions where the correlation length of concentration fluctuations ξ does not exceed ξ_{cross}, the Landau description of critical phenomena in polymer mixtures is selfconsistent ("Ginzburg criterion"[21, 22, 18]).

where b is the length of an effective segment and $N_A = N_B = N$ the number of segments, Tang *et al.*[15] find $T_c(\infty) - T_c(D) \propto D^{-1}$ instead. An implicit assumption made by Tang *et al.* is that the film thickness D is large enough to leave the three-dimensional Gaussian-like configurations of the single polymer coils (i.e., coil size $\propto\sqrt{N}$) unperturbed. Raphael,[17] on the other hand, considers the case of ultrathin films ($D \ll \sqrt{N}$), where the chains are strongly compressed and essentially exhibit two-dimensional behavior.

The mean-field study of Tang *et al.*[15] only applies to the crossover from regime I to regime II. This crossover is less interesting than that from regime III to regime IV, since the critical exponents of mean field theory do not depend on the spatial dimension d, whereas they do for the Ising universality class. Therefore we study the latter crossover in the present work, which is, however, not only of theoretical, but also of practical interest because the shape of the miscibility gap between the two coexisting phases with volume fraction $\phi^{(2)}_{\text{coex}}$, $\phi^{(1)}_{\text{coex}}$ of species A obeys

$$\phi^{(2)}_{\text{coex}} - \phi^{(1)}_{\text{coex}} = \hat{B}(D)[1 - T/T_c(D)]^{\beta} \qquad \text{for} \quad T \leqslant T_c(D) \tag{3}$$

In Eq. (3) $\hat{B}$ is a "critical amplitude"[23] and β is the critical exponent of the order parameter, which depends on the dimensionality of space in general. While Landau theory[23] as well as Flory–Huggins theory of polymers blends in the bulk[24,25] fix[26] $\beta = 1/2$, the universality principle[23,27] implies that the bulk behavior of polymer blends near $T_c(\infty)$, where the correlation length ξ exceeds ξ_{cross} (see footnote 4), is Ising-like, i.e., β has the value[28]

$$\beta = \beta_3 \approx 0.325 \tag{4}$$

of the three-dimensional Ising model. Both simulations[2,29] and recent experiments[30] have shown that the Ising regime is easily observable over a wide range of chain lengths, and one has to go to *very large* N to establish mean-field critical behavior. However, two-dimensional criticality is expected when ξ exceeds D, which is easily reached for polymer blends, since in the bulk ξ has a very large critical amplitude prefactor $\hat{\xi}$,[18]

$$\xi = \hat{\xi}(N)[1 - T/T_c(\infty)]^{-\nu_3}, \qquad \hat{\xi} \approx bN^{1-\nu_3} \tag{5}$$

where $\nu_3 \approx 0.63$[28] is the correlation length exponent of the three-dimensional Ising model. For $\xi > D$ we then expect Eq. (3) to hold with[23]

$$\beta = \beta_2 = 1/8 \tag{6}$$

While the Landau theory of Tang *et al.*[15] implies a parabolic shape of the coexistence curve throughout, i.e., $\beta = 1/2$, Kumar *et al.*[16] use Eq. (4) even

for very thin films. Since they studied only two thicknesses and found $T_c(D)$ from an extrapolation where Eq. (3) with $\beta = \beta_3$ is fitted to their data, only a preliminary test of Eq. (1) has been possible.

The aim of the present work is a Monte Carlo study of the coexistence curve in thin polymeric films with particular emphasis on a proper description of the crossover in the critical behavior and the shift of the critical point with thickness. While for the Ising model such a study was already presented 20 years ago,[10] our work is the first of its kind for polymer mixtures. Section 2 briefly recalls the model and simulation technique, while Section 3 discusses the analysis of our data in terms of suitable crossover scaling concepts.[31, 32] Section 4 presents our phase diagrams and concludes with a discussion and outlook on more general situations.

2. MODEL AND SIMULATION TECHNIQUE

As in previous studies of symmetrical polymer mixtures in the bulk[18, 19] we use a simple cubic lattice and represent polymer chains by "effective monomers" blocking all eight sites of an elementary cube from further occupation. These "monomers" are connected by "effective bonds" whose lengths may take the values $b = 2, \sqrt{5}, \sqrt{6}, 3$, and $\sqrt{10}$ (all lengths being measured in units of the lattice spacing). We work at a volume fraction $\phi_v = 0.5$ of vacant sites, since various criteria show that the corresponding monomer density already represents a melt density,[33, 34] but on the other hand the acceptance rates for the moves of our dynamic Monte Carlo algorithm[5] are still fairly high. These moves are a mixture of random hopping of single monomers[33] and "slithering snake"-type[35, 36] moves in analogy to ref. 37, since in this way one reaches a rather fast equilibration of the chain configurations.[37]

All our data are for a single chain length $N = 32$. When comparing this choice to experiment, one should recall that we work with a coarse-grained model which can be thought of as integrating $n = 3$–5 successive chemical bonds along the backbone of a real polymer chain into one effective bond of the model.[38] This choice of model is legitimate as the unmixing transition of polymer blends deals with long-wavelength phenomena [cf. Eq. (5)] and the unrealistic details on the scale of b hence should not matter. Since $N \triangleq 32$ corresponds to a degree of polymerization of about $N_p = 100$ to $N_p = 150$, the study of longer chains would clearly be desirable. However, this is not done here, since previous work[18, 19] has shown that one does *only* find pure (three-dimensional) Ising critical behavior in the

[5] See ref. 35 for a general discussion of Monte Carlo mehods for lattice models of polymers.

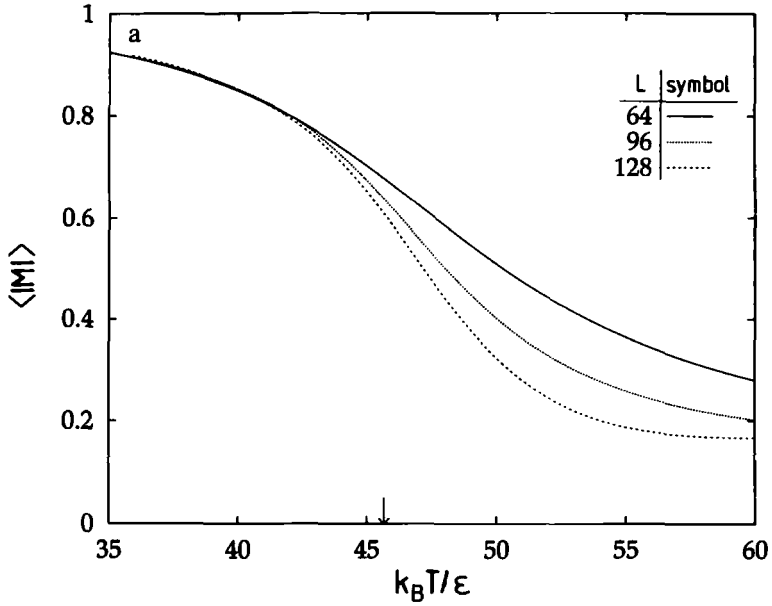
a
L | symbol
64
96
128
⟨|M|⟩
k_BT/ε
0
0.2
0.4
0.6
0.8
1
35
40
45
50
55
60

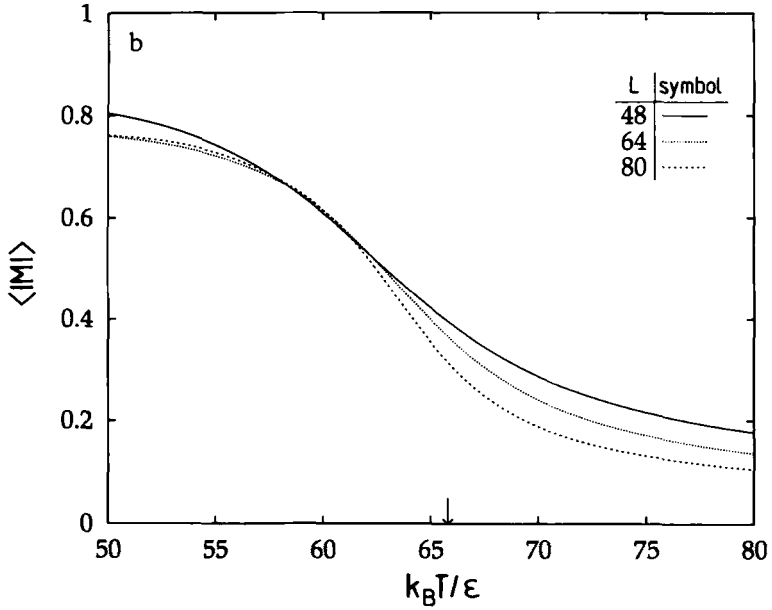
b
L | symbol
48
64
80
⟨|M|⟩
k_BT/ε
0
0.2
0.4
0.6
0.8
1
50
55
60
65
70
75
80

bulk for $N \leqslant 32$. For $N \geqslant 64$ one has entered the regime where a gradual crossover to mean-field behavior sets in, which extends over several decades in chain length.[18, 30] We wish to avoid the complications of dealing simultaneously with multiple crossovers here, although it is well possible that such phenomena will be relevant for experiments. Therefore we restrict attention to short enough chains that are strictly Ising-like in the bulk.

As in a previous work,[19, 39] we chose a square-well-type potential between monomers in its most symmetrical form ($\varepsilon_{AB} = -\varepsilon_{AA} = -\varepsilon_{BB} = \varepsilon$) with an interaction range $\sqrt{6}$. This means that all neighbors within the first peak of the radial distribution function contribute to these interactions.[39] As usual,[19, 29] we work in the semi-grand canonical ensemble, where temperature and chemical potential difference $\Delta_\mu = \mu_A - \mu_B$ between A and B monomers are the independent control parameters. In addition to the moves to relax the chain configurations as described above, one then also needs moves where A chains are transferred into B chains of fixed configuration (or vice versa). Being interested in the coexistence curve and considering "neutral" walls (i.e., there are no wall chemical potentials acting on A or B monomers present), the simulations are in fact carried out exclusively at $\Delta\mu = 0$.

Our lattice geometry then is $L \times L \times D$ with two free (repulsive) $L \times L$ surfaces and periodic boundary conditions in the other lattice directions parallel to the walls. Monomers cannot cross the walls, but in other respecter these walls only have the effect of "missing neighbors" for monomers close to this wall (i.e., within the interaction range). In other work[40] a short-range preferential attraction between the walls and one of the species was introduced in order to test theoretical concepts on surface enrichment and wetting phenomena.[41] This is not done here. Also we do not assume any change of the strength (or range, respectively) of the pairwise interaction ε near the free surfaces (by a strong enough surface enhancement of ε, one may reach a situation where phase separation at the surfaces in a two-dimensional geometry sets in at a temperature where the bulk is still miscible; see corresponding studies of Ising models).[8, 42, 43]

In this simulation we focus on the finite-size effect due to the finite thickness D of the film only. The film thickness takes the values $D = 8$,

---

Fig. 2. Average value of the order parameter $\langle |M| \rangle$ plotted vs. reduced temperature $k_B T/\varepsilon$ for (a) $D = 10$ and (b) $D = 36$. Several choices of L are included as indicated in the figure. Note that the curves are smooth for *any* finite value of L. Only for $L \to \infty$ is Eq. (3) expected to be found. The arrow indicates the critical temperature $T_c(D)$ in the limit $L \to \infty$, as results from the cumulant intersection method described in the text (see Fig. 4).

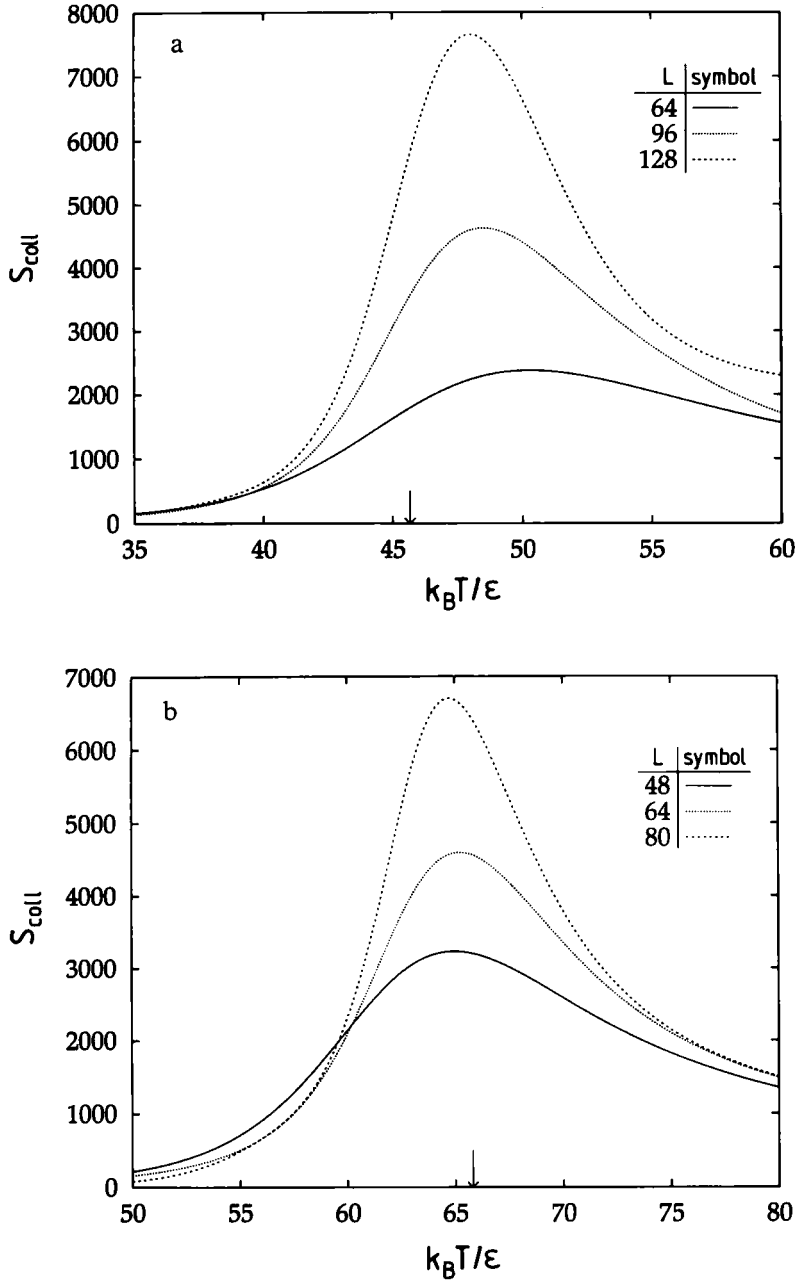

Fig. 3. Same as Fig. 2, but for the collective scattering function $S_{coll} = L^2 D[\langle M^2 \rangle - \langle |M^2| \rangle^2]$. Again the function is smooth for any finite value of L.

10, 12, 14, 16, 20, 24, 28, 36, and 48 in our studies. Since Monte Carlo simulations deal with systems which are finite in all linear dimensions, the effects due to the finite linear dimension L in the direction parallel to the wall have to be disentangled from the thickness effects in which we are interested here. This can be done by studying at every value of D a sequence of values of L—in practice we use mostly $L=48$, 64, and 80, but occasionally also other sizes (up to $L=352$ for $D=8$, up to $L=128$ for $D=10$ and $D=14$) were considered as well—and by carrying out a finite-size scaling extrapolation to $L\to\infty$ at fixed D. This finite-size scaling analysis[9, 19, 24, 44] in principle works as for the analysis of phase separation in the bulk. In practice the accuracy is somewhat limited here due to the problem of crossover from three-dimensional to two-dimensional criticality, as discussed in the next section.

For generating the "raw Monte Carlo data" for this analysis, we carried out a run at three temperatures in the critical region with about 320,000 Monte Carlo steps per monomer each (independent configurations are obtained after about 60 MCS), which were used as input for a "multi-histogram" interpolation[19] to obtain data as shown in Figs. 2 and 3 for the moments of the order parameter M of the thin films defined as

$$M := (n_A - n_B)/(n_A + n_B) \tag{7}$$

where n_A is the number of A chains and n_B the number of B chains in the system. Remember that our semi-grand canonical simulation algorithm keeps the total number $n = n_A + n_B$ of chains fixed, while their difference is fluctuating. We estimate that the statistical accuracy of our data for $\langle |M| \rangle$ and $\langle |M^2| \rangle$ is better than 1% relative error. Note further that in a symmetrical mixture the volume fractions $\phi_{A,B}$ of A and B monomers (i.e., $\phi_{A,B} = 8Nn_{A,B}/L^2D$; 8 is number of lattice sites occupied by one monomer in the bond-fluctuation model) at the coexistence curve are related to $\langle |M| \rangle$ via[19, 26, 29]

$$\frac{\phi_A}{1-\phi_v} = \frac{1}{2}(1 + \langle |M| \rangle), \qquad \frac{\phi_B}{1-\phi_v} = \frac{1}{2}(1 - \langle |M| \rangle) \qquad \text{for} \quad L \to \infty \tag{8}$$

The choice of signs in Eq. (8) implies that we consider only the A-rich part of the phase diagram. For symmetrical mixtures the phase diagram exhibits mirror symmetry in the plane of variables $(T, \phi := \phi_A/[1-\phi_v])$ around the line $\phi = 1/2$. Hence the behavior of the B-rich part of the phase diagram is simply obtained by interchanging the labels A, B in Eq. (8).

From Fig. 2 it is evident that for finite L the order parameter $\langle |M| \rangle$ is a smooth function of temperature. Thus one cannot straightforwardly infer the temperature $T_c(D)$, where the order parameter vanishes for $L\to\infty$ [see Eq. (3)], and neither the exponent β nor the amplitude factor

$\hat{B}(D)$ can immediately be determined. However, finite-size scaling[19, 29, 44] implies that reduced moment ratios with $ij = kl$

$$U_{ij}^{kl}(T, L) := \langle |M|^k \rangle^l / \langle |M|^i \rangle^j \tag{9}$$

near $T_c(D)$ should depend on the ratio L/ξ only, when $\xi \gg D$, so that one deals with the limiting two-dimensional critical behavior

$$U_{ij}^{kl}(T, L) = \tilde{U}_{ij}^{kl}(L/\xi) \to \tilde{U}_{ij}^{kl}(0) \qquad \text{for} \quad T \to T_c(D) \tag{10}$$

Equation (10) implies that ultimately (i.e., for large enough L) all curves $U_{ij}^{kl}(T, L)$ when plotted as function of T for different L must intersect in a common intersection point $\tilde{U}_{ij}^{kl}(0)$, and the temperature for which this happens is $T_c(D)$. Figure 4 shows a test of this concept for $D = 10$. Whereas Eq. (10) yields a very precise estimate of $T_c(D)$ for $D = 10$, there is considerable scatter of the intersection points for larger film thicknesses and thus $T_c(D)$ can be estimated with this method only with a relative accuracy of about 1% in general. This is much worse than for bulk three-dimensional problems,[19, 29] where a relative accuracy of 0.1% (or even better)

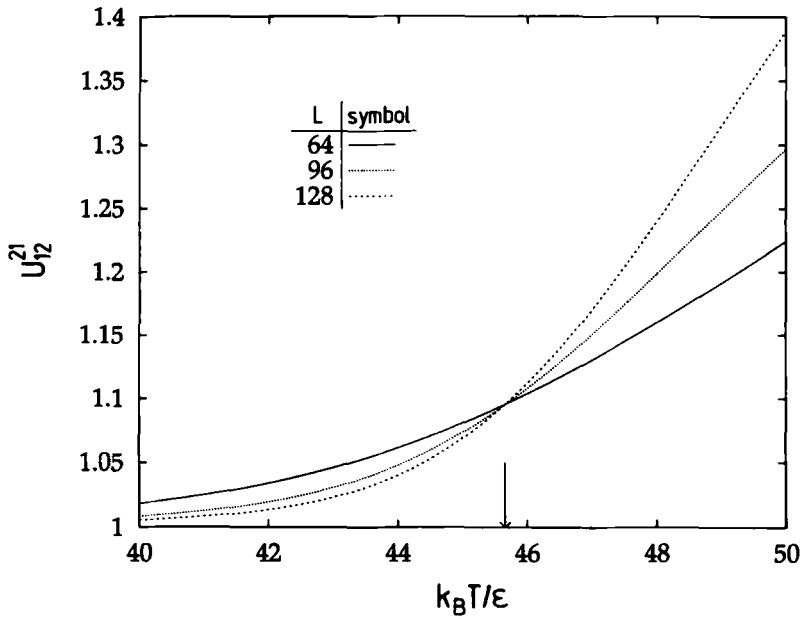

Fig. 4. Plot of U_{12}^{21} versus inverse temperature for $D = 10$ for several different sizes in the temperature region near $T_c(D)$. The intersection point, denoted by a down-pointing arrow, yields $T_c(D)$ (see text for further details).

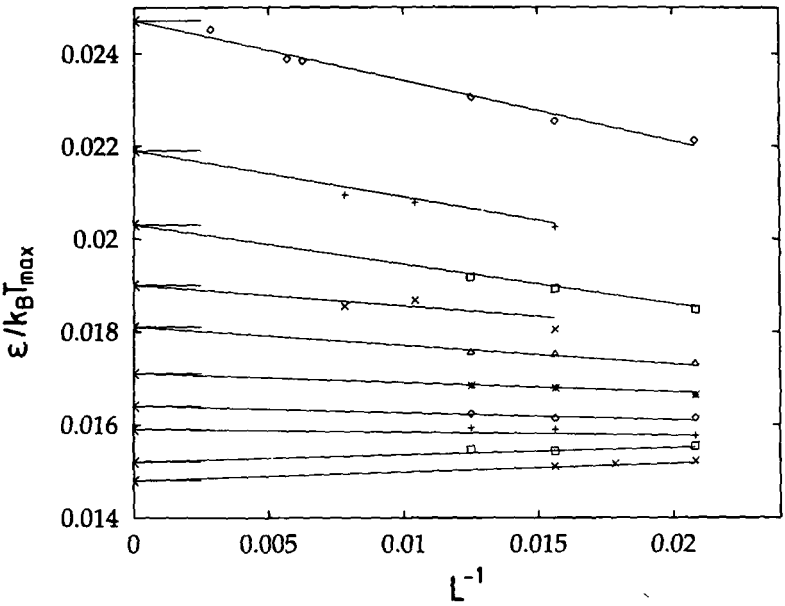

Fig. 5. Plot of the inverse temperature $\varepsilon/k_B T_{max}$ of the maximum S_{max} of the collective scattering function S_{coll} (Fig. 3) versus L^{-1} [see Eq. (12)]. From the top to the bottom the data points correspond to $D = 8$, 10, 12, 14, 16, 20, 24, 28, 36, and 48, respectively. Arrows show the estimates $\varepsilon/k_B T_c(D)$ of the cumulant intersection method (see Fig. 4 for details), which are collected in Table I. The straight lines through the data points $\varepsilon/k_B T_{max}$ are best fits with the constraint that the limit $L \to \infty$ yields $\varepsilon/k_B T_c(D)$.

could be reached. However, this difficulty is inevitable here due to the crossover from three- to two-dimensional criticality, which is felt as long as the ratio L/D is finite .[31, 32]

An alternative method[44] to estimate $T_c(D)$ is to extrapolate the location of the point where the collective scattering junction S_{coll} is maximal (Fig. 5). Remember that S_{coll}, defined as (cf. Fig. 3)

$$S_{coll} = L^2 D[\langle M^2 \rangle - \langle |M| \rangle^2] \tag{11}$$

for $T < T_c(D)$, describes the intensity of scattering from concentration fluctuations for states at the coexistence curve of the mixture .[19, 29] One expects that the temperature of the maximum T_{max} scales as

$$T_{max}(L, D) - T_c(D) \propto L^{-1/\nu} \qquad \text{for} \quad L \to \infty \tag{12}$$

where $\nu = \nu_2 = 1$ is the two-dimensional value of the correlation length exponent. Of course, Eq. (12) is supposed to be valid for large enough

Table I. Dependence of the Critical Temperature T_c on the Film Thickness D

D	$\varepsilon/k_B T_c$
∞	0.0142486[19]
48	0.0148 ± 0.00015
36	0.0152 ± 0.00015
28	0.0159 ± 0.00016
24	0.0164 ± 0.00016
20	0.0171 ± 0.00017
16	0.0181 ± 0.00018
14	0.019 ± 0.00019
12	0.0203 ± 0.0002
10	0.0219 ± 0.00022
8	0.02471 ± 0.00025

"aspect ratio" $L/D \gg 1$, which is not really reached for our larger values of D. Therefore the accuracy of our final estimates for $T_c(D)$ (see Table I) deteriorates with increasing D, and no attempt was made to locate any transition for $D > 48$.

3. DIMENSIONAL CROSSOVER AND FINITE-SIZE SCALING

Given the estimates for $T_c(D)$, one can try to fit data such as shown in Figs. 2 and 3 to finite-size scaling forms such as[19, 44]

$$\langle |M| \rangle L^v = \tilde{M}(L^u t) \qquad \text{with} \quad t = |1 - T/T_c(D)| \tag{13}$$

where u, v are "effective exponents" determined such that an optimal collapse of the family of curves $\langle |M| \rangle$ for all L onto a "master curve" $\tilde{M}(z)$ is obtained. While for a three-dimensional Ising system (i.e., $L, D \to \infty$) the theory[9, 19, 44] implies $v = \beta_3/\nu_3$, $u = 1/\nu_3$, we expect here for $L \to \infty$ and D fixed (i.e., large aspect ratios L/D) a two-dimensional behavior, i.e., $v = \beta_2/\nu_2$, $u = 1/\nu_2$.

As already mentioned above, the aspect ratios L/D studied were not large enough to exhibit the two-dimensional critical behavior clearly. As a consequence, it is better not to fix u, v to their theoretical values, but rather allow for "effective exponents" which smoothly interpolate between the two- and three-dimensional values. Such "effective exponents" have a well-defined meaning even in the framework of a renormalization group description of dimensional crossover.[45] Figure 6 shows, as an example, data for $D = 16$ and $D = 36$. It is seen that within some scatter a fairly reasonable "data collapsing"[44] is obtained. Since the idea[45] that such effective

Table II. Effective Exponents and Critical amplitudes[a]

D	u	v	β_{eff}	w	γ_{eff}	ν_{eff}	$\hat{B}_{\text{eff}}$	d_{eff}
2-dim	1	1/8	1/8	7/4	7/4	1	—	2
8	0.913	0.174	0.191	1.807	1.979	1.095	—	2.16
10	1.149	0.156	0.136	1.741	1.514	0.870	1.17	2.05
12	1.196	0.161	0.135	1.706	1.427	0.836	1.11	2.03
14	1.255	0.207	0.165	1.756	1.400	0.797	1.38	2.17
16	1.398	0.241	0.172	1.621	1.160	0.716	1.53	2.10
20	1.302	0.273	0.210	1.564	1.201	0.768	1.20	2.11
24	1.186	0.259	0.219	1.474	1.243	0.843	1.26	1.99
28	1.203	0.285	0.237	1.489	1.238	0.831	1.43	2.06
36	1.211	0.366	0.302	1.355	1.119	0.826	1.62	2.09
48	1.128	0.390	0.346	1.300	1.153	0.886	1.56	2.08
∞	1.587	0.516	0.325	1.970	1.241	0.630	—	3

[a] For $D = 8$ the size of the radius of gyration is comparable to the film thickness, which prevents a determination of $\hat{B}_{\text{eff}}$ (see text for further details).

exponents have physical significance and satisfy the standard scaling relations among critical exponents[23,27] implies that the effective order parameter exponent β_{eff} can be defined as

$$\beta_{\text{eff}} = v/u \tag{14}$$

we can also estimate the corresponding "effective" amplitude $\hat{B}_{\text{eff}}(D)$ [cf. Eq. (3)] by fitting the scaling function $\tilde{M}(z = L^u t)$ in Eq. (13) for large z as

$$\tilde{M}(z \gg 1) = \hat{B}_{\text{eff}}(D)\, z^{\beta_{\text{eff}}} \tag{15}$$

and in this way estimates for $\tilde{B}_{\text{eff}}$ are obtained in addition. Apart from an (extremely narrow) region around the critical temperature $T_c(D)$ where Eq. (3) holds with the true two-dimensional value $\beta_2 = 1/8$, a complete description of the coexistence curve thus becomes possible, since Eqs. (13) and (15) imply that for $L \to \infty$

$$\langle |M| \rangle = \hat{B}_{\text{eff}}(D)\, t^{\beta_{\text{eff}}} \tag{16}$$

Table II collects our estimates for the effective exponents and amplitudes. There we have also analyzed the collective scattering function S_{coll}

$$S_{\text{coll}} L^w = \tilde{S}(L^u t) \tag{17}$$

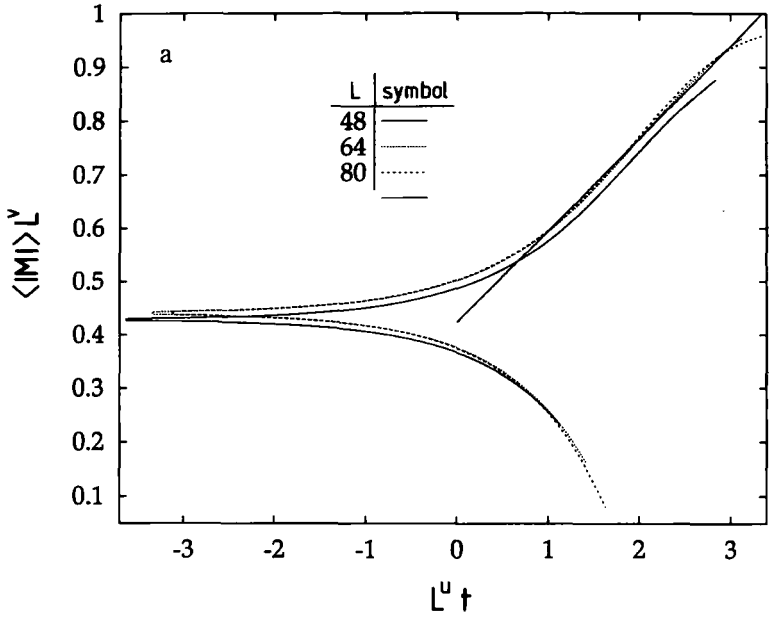
a
L | symbol
48
64
80
1
0.9
0.8
0.7
0.6
0.5
0.4
0.3
0.2
0.1
-3
-2
-1
0
1
2
3
⟨|M|⟩L^ν
L^u t

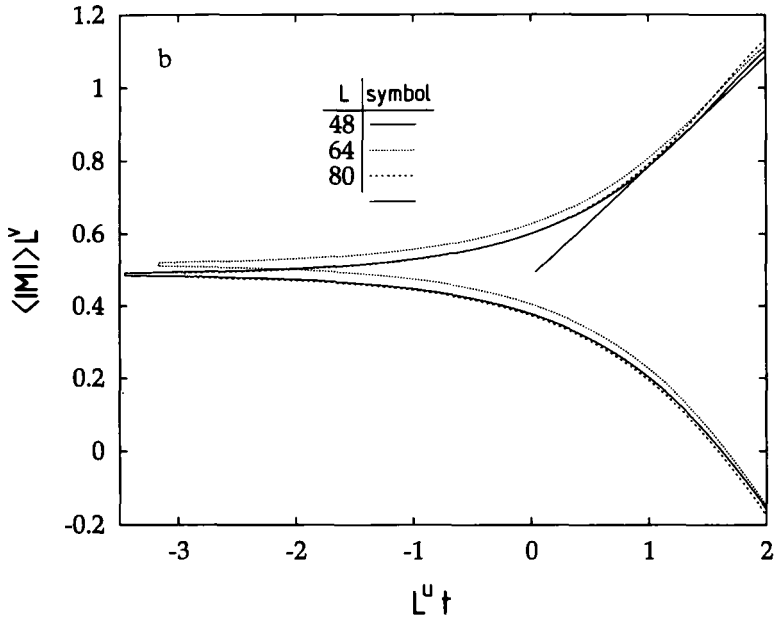
b
L | symbol
48
64
80
1.2
1
0.8
0.6
0.4
0.2
0
-0.2
-3
-2
-1
0
1
2
⟨|M|⟩L^ν
L^u t

Corresponding to the discussion following Eq. (13), one expects the exponent w to cross over from $w=\gamma_3/\nu_3$ in $d=3$ to $w=\gamma_2/\nu_2$ in $d=2$. Hence we define

$$\gamma_{\text{eff}}=w/u \tag{18}$$

in analogy to Eq. (14). Both w and γ_{eff} are included in Table II, as well as an "effective dimensionality" d_{eff} defined from a hyperscaling relation[45] [remember $d=(2\beta+\gamma)/\nu$][27]

$$d_{\text{eff}}=(2\beta_{\text{eff}}+\gamma_{\text{eff}})/\nu_{\text{eff}}=2v+w \tag{19}$$

It should be stressed that the effective exponents in Table II have a relative accuracy presumably of about 10% only, due to a variety of errors—inaccuracy of T_c, ambiguity of the fits to Eqs. (13) and (17), and statistical errors in the raw data. Discarding thus the data for $D=8$—which may be anomalous, since for $N=32$ the radius of gyration ($\langle R_g^2\rangle^{1/2}\approx 7^{(33)}$) is of the same order as the film thickness—both β_{eff} and γ_{eff} are compatible with the expected behavior, namely a smooth interpolation between the two-dimensional (for small D) and the three-dimensional values (for larger D). However, $\nu_{\text{eff}}=1/u$ shows a surprising nonmonotonic variation: while the decrease with increasing D for small D is expected the increase for $D\geqslant 20$ is unexpected. Also d_{eff} stays close to $d=2$ throughout, rather than interpolating between $d=2$ and $d=3$ smoothly, as suggested in ref. 45. Thus either the systematic errors in our procedures are distinctly larger than estimated, or the dimensional crossover in polymer blend films has some unexpected features.

A somewhat more systematic description of dimensional crossover can be derived as follows.[31, 32] Instead of working with Eq. (13) we formulate a scaling assumption in terms of the variables $t_\infty := 1-T/T_c(D=\infty)$ and L, i.e.,

$$\langle |M|^k\rangle = D^{-k\beta_3/\nu_3}\bar{M}_k(L/D,\, D^{1/\nu_3}t_\infty) \tag{20}$$

Since Eq. (20) formulates the finite size scaling with respect to the bulk three-dimensional critical point $T_c(D=\infty)$, the three-dimensional

---

Fig. 6. Log-log plot of $\langle |M|\rangle L^v$ versus $z:=L^u t$, for (a) $D=16$ and (b) $D=36$. Three choices of L are included as indicated. For $D=16$ the choices for the effective exponents are $u=1.40$ and $v=0.241$, and for $D=36$ they are $u=1.21$ and $v=0.366$. The solid straight lines at the upper branch of the scaling functions represent its asymptotic behavior, $\bar{M}(z\gg 1)=\hat{B}(D)\, z^{\beta_{\text{eff}}}$, where for $D=16$, $\beta_{\text{eff}}=0.172$ and $\hat{B}(D)=1.53$, while for $D=36$, $\beta_{\text{eff}}\approx 0.303$ and $\hat{B}\approx 1.56$. Note that the lower branch of the scaling functions $\langle |M|\rangle L^v$ describes temperatures $T>T_c(D)$ and is of no interest here.

exponents have to be used. This scaling assumption is valid if both L and D are very large, whereas the aspect ratio L/D may be arbitrary. Using Eq. (11), we derive from Eq. (20) an analogous scaling expression for the scattering function

$$S_{\text{coll}} = D^{\gamma_3/\nu_3} \bar{S}(L/D, D^{1/\nu_3} t_\infty) \tag{21}$$

by defining $\bar{S} := (L/D)^2(\bar{M}_2 - \bar{M}_1^2)$ and using the hyperscaling relation $\gamma_3 + 2\beta_3 = 3\nu_3$.

From Eqs. (20) and (21) one can justify Eq. (1) and additionally derive the dependence of $\langle |M| \rangle$ and of S_{coll} on L. In order to obtain Eq. (1), let us consider the limit $L \to \infty$ at *fixed* D. In this limit two-dimensional criticality emerges as the singularity of the scaling functions when the second argument $y = D^{1/\nu_3} t_\infty$ reaches a critical value $y_c := y(T_c(D))$,

$$\langle |M| \rangle \propto D^{-\beta_3/\nu_3} (y - y_c)^{\beta_2} = D^{(\beta_2 - \beta_3)/\nu_3} (t_\infty - t_{\infty,c})^{\beta_2} \tag{22}$$

$$S_{\text{coll}} \propto D^{\gamma_3/\nu_3} (y - y_c)^{-\gamma_2} = D^{(\gamma_3 - \gamma_2)/\nu_3} (t_\infty - t_{\infty,c})^{-\gamma_2} \tag{23}$$

The relation

$$y_c = y(T_c(D)) = D^{1/\nu_3} t_{\infty,c} \tag{24}$$

implies

$$T_c(\infty) - T_c(D) = T_c(\infty)\, y_c D^{-1/\nu_3} \propto D^{-1/\nu_3} \tag{25}$$

i.e., Eq. (1). In addition, Eqs. (22) and (23) immediately yield the D dependence of the amplitude $\hat{B}(D)$ of the order parameter and of the amplitude $\hat{\Gamma}(D)$ of the collective structure function

$$\hat{B}(D) \propto D^{(\beta_2 - \beta_3)/\nu_3} \approx D^{-0.317}, \qquad \hat{\Gamma}(D) \propto D^{(\gamma_2 - \gamma_3)/\nu_3} \approx D^{0.81} \tag{26}$$

In order to derive the dependence of $\langle |M| \rangle$ and of S_{coll} on L, we fix y at its value at $T_c(D)$, i.e., at $y = y_c$ and calculate the variation of $\langle |M| \rangle$ and of S_{coll} with L. Defining

$$\bar{M}_k(L/D, y_c) = \bar{\bar{M}}_k(L/D) \qquad \text{and} \qquad \bar{S}(L/D, y_c) = \bar{\bar{S}}(L/D) \tag{27}$$

we can rewrite Eqs. (20) and (21) as follows:

$$\langle |M| \rangle (T = T_c(D)) = D^{-\beta_3/\nu_3} \bar{\bar{M}}_1(L/D) \tag{28}$$

$$S_{\text{coll}}(T = T_c(D)) = D^{\gamma_3/\nu_3} \bar{\bar{S}}(L/D) \tag{29}$$

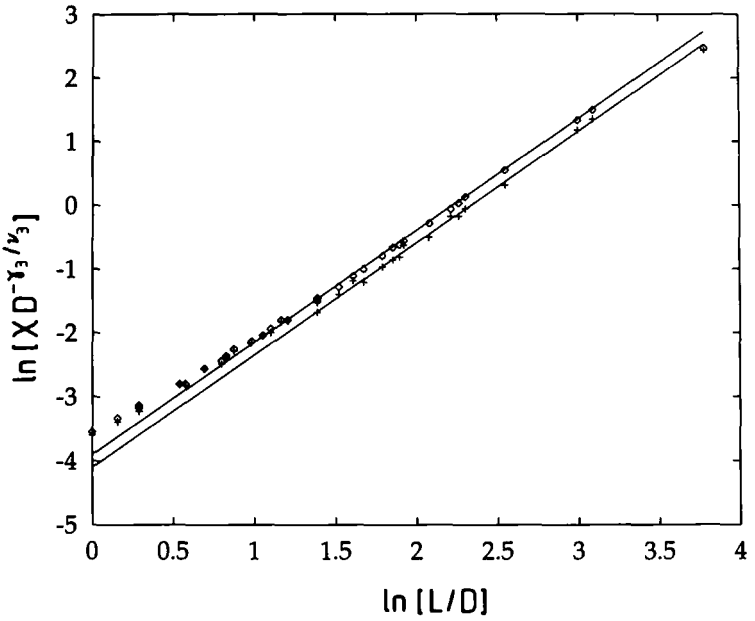

Fig. 7. Log-log plot of $\chi(T-T_c(D))\,D^{-\gamma/\nu_3}$ (crosses) and $\chi_{\max}D^{-\gamma_3/\nu_3}$ (diamonds) versus L/D (note that the "susceptibility" χ is related to the scattering function via $\chi = S_{\text{coll}}\varepsilon/k_B T$). Both straight lines have the theoretical slope of $\gamma_2/\nu_2 = 1.75$.

For large L, Eqs. (28) and (29) must become compatible with Eqs. (13) and (17), where the exponents u, v, and w take their two-dimensional values (i.e., $u=\beta_2/\nu_2$, $v=1/\nu_2$, $w=\gamma_2/\nu_2$). This implies that $\bar{\bar{M}}_1(L/D \gg 1) \propto (L/D)^{-\beta_2/\nu_2}$, and similarly $\bar{\bar{S}} \propto (L/D)^{\gamma_2/\nu_2}$. Thus we predict that at $T=T_c(D)$ for large L/D the order parameter and the scattering function scale as

$$\langle |M| \rangle (T=T_c(D)) \propto \langle |M| \rangle (T=T_{\max}) \propto D^{\beta_2/\nu_2-\beta_3/\nu_3} L^{-\beta_2/\nu_2} \tag{30}$$

$$S_{\text{coll}}(T=T_c(D)) \propto S_{\text{coll}}(T=T_{\max}) \propto D^{\gamma_3/\nu_3-\gamma_2/\nu_2} L^{\gamma_2/\nu_2} \tag{31}$$

Here we have used the fact that the same scaling also applies at the position $T_{\max}$ of the maximum of the scattering function. Equations (25), (30), and (31) are the major predictions of the presented scaling theory.

Before testing these predictions in our simulation we want to show the internal consistency of our approach by the following consideration. Noting that the correlation length ξ scales as [cf. Eqs. (20)–(23)]

$$\xi = D\bar{\xi}(L/D, D^{1/\nu_3}t_\infty) \xrightarrow{L\to\infty} D^{1-\nu_2/\nu_3}(t_\infty - t_{\infty,c})^{-\nu_2} \tag{32}$$

we see that the Eqs. (22) and (23) reduce to Eqs. (30) and (31) when putting $\xi \approx L$ in Eq. (32). In addition, since the second moment $\langle M^2 \rangle$ at $T = T_c(D)$ or at T_{max} scales analoguously,

$$\langle M^2 \rangle (T = T_c(D)) \propto \langle M^2 \rangle (T = T_{max}) \propto D^{2(\beta_2/\nu_2 - \beta_3/\nu_3)} L^{-2\beta_2/\nu_2} \quad (33)$$

Eq. (11) implies

$$S_{coll}(T = T_c(D)) \propto S_{coll}(T = T_{max}) \propto L^2 D^{1-2\beta_3/\nu_3} = D^{3-2\beta_3/\nu_3} (L/D)^{2-2\beta_2/\nu_2} \quad (34)$$

If one uses the hyperscaling relations $3 - 2\beta_3/\nu_3 = \gamma_3/\nu_3$ and $2 - 2\beta_2/\nu_2$ one sees that Eq. (34) is also compatible with Eq. (31). Therefore both Eqs. (30) and (31) may be derived from the scaling assumption of the correlation length, which shows the internal consistency of presented theoretical description.

This crossover scaling description is now tested in Figs. 7 and 8. While for the "susceptibility" χ ($\chi = S_{coll} \varepsilon / k_B T$ is the response function $\partial \langle M \rangle / \partial H$

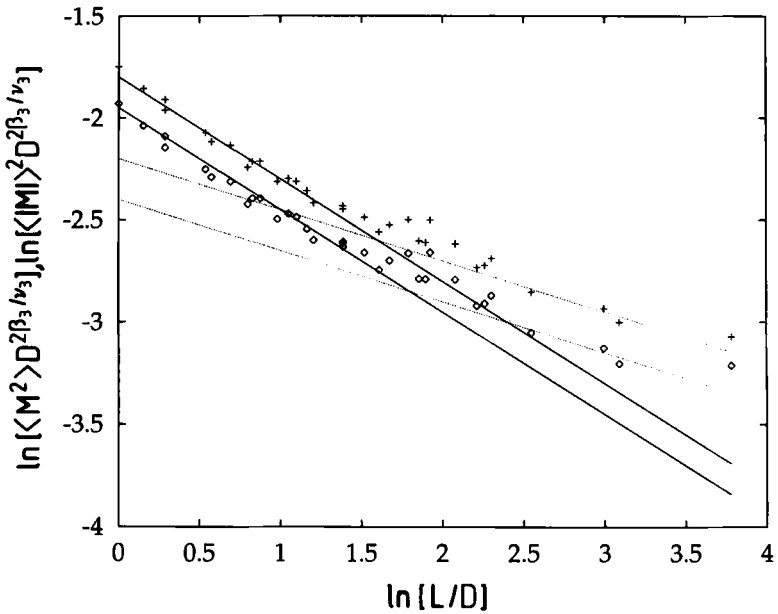

Fig. 8. Log-log plot of $\langle M^2 \rangle (T = T_{max})\, D^{2\beta_3/\nu_3} \varepsilon / k_B T_{max}$ (crosses) and $(\langle |M| \rangle\, D^{\beta_3/\nu_3})^2 \varepsilon / k_B T_{max}$ (diamonds) versus L/D. Straight lines for small L/D have slope 1/2, while the straight lines for L/D large also have the theoretical slope $2\beta_2/\nu_2 = 0.25$.

with respect to the conjugated "field" H for an Ising magnet) the data collapsing suggested by Eq. (29) seems quite perfect, and the expected two-dimensional criticality [see Eq. (31)] is rapidly approached, there is more scatter for the individual moments $\langle |M| \rangle^2$, $\langle M^2 \rangle$ (Fig. 8). Also, for $\ln(L/D) \leqslant 2$ a power law with twice the expected slope appears, which is unexpected. Only for $\ln(L/D) \geqslant 2$ do we see the expected behavior, Eqs. (30) and (33). Thus it is less of a surprise that for $D \geqslant 20$ [where the region $\ln(L/D) \geqslant 2$ was not reached] the effective exponents in Table II do not fully show the expected trend yet.

There is some arbitrariness in whether one should analyze $\chi = S_{\text{coll}} \varepsilon / k_B T$ or S_{coll} itself. In principle, for large enough film thicknesses all data would lie so close to the critical point that one could replace $\varepsilon/k_B T$ by $\varepsilon/k_B T_c$ with negligible error. Unfortunately, part of our data are rather far away from $T_c(D)$, and hence the scaling plots using $\chi(T = T_{\max})$ and $S_{\text{coll}}(T = T_{\max})$ are not strictly equivalent. Since we have found that the scaling plot for χ is presumably closer to the asymptotic behavior, this plot is shown in Figs. 7 and 8.

4. DISCUSSION OF THE CRITICAL POINT SHIFT AND OF THE PHASE DIAGRAMS

Figure 9 tests Eqs. (1) and (25). It is seen that the expected behavior is compatible with the data for $D \geqslant 20$ only. This is not a surprise, since for $D \leqslant 16$ the shift of T_c is relatively large, $1 - T_c(D)/T_c(\infty) \geqslant 0.2$, and thus the system is really outside of the critical region, where the three-dimensional Ising critical behavior dominates. If we used the mean-field theory for the description of the shift of $T_c(D)$, the result for the correlation length[26] $\xi = \langle R_g^2 \rangle^{1/2} [1 - T/T_c(\infty)]^{-1/2}$ implies that at $T_c(D = 16)$ the bulk correlation length of a three-dimensional blend would only be about twice as large as the radius of gyration, namely $\xi \approx 15$ for $N = 32$. A possible interpretation of the small-D behavior of Fig. 9 then is to assume that the crossover length ξ_{cross} [see Eq. (2)] is of this order, since we expect $T_c(\infty) - T_c(D) \propto D^{-1}$ for $D \leqslant \xi_{\text{cross}}$,[15] in the regime of mean-field critical behavior. Note that Tang *et al.*[15] estimated the prefactor of Eq. (15) to be about 0.2. Assuming thus $\xi_{\text{cross}} \approx 0.2bN$ with $N = 32$ and $b \approx 2.7$[33] yields $\xi_{\text{cross}} \approx 17$. This estimate reinforces the conclusion that our data for small D fall in the regime $D < \xi_{\text{cross}}$. Although the shift of T_c can thus be described by the mean-field relation $T_c(\infty) - T_c(D) \propto D^{-1}$ for $D \leqslant \xi_{\text{cross}}$ for small D, the critical behavior near $T_c(D)$ is a two-dimensional Ising behavior. In the picture of Fig. 1, a variation of T at constant N corresponds to a move parallel to the abcissa. When D is small, the broken

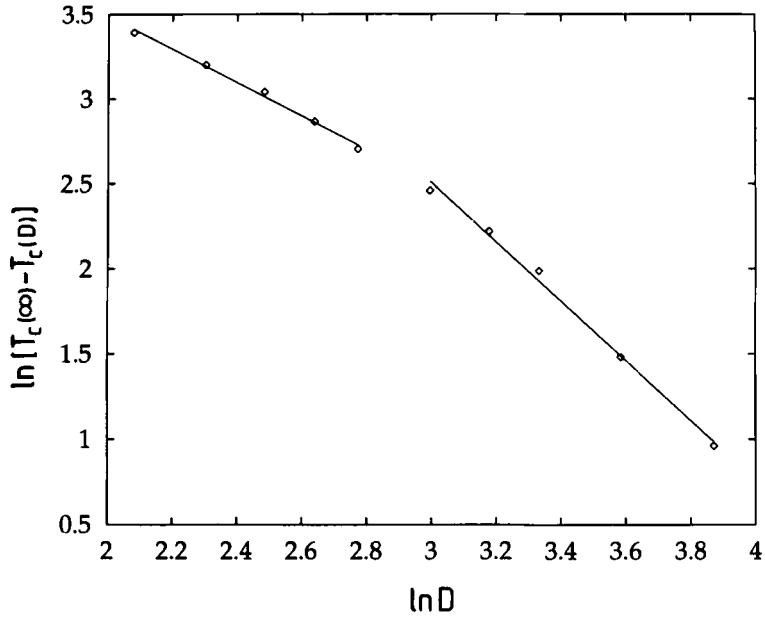

Fig. 9. Log-log plot of $T_c(\infty) - T_c(D)$ versus D. For small D, the straight line corresponds to a shift $T_c(\infty) - T_c(D) \propto 1/D$, while the second straight line for larger D shows Eq. (25) with $\nu_3 = 0.63$.

straight line is close to the ordinate axis, and there is only a small regime of three-dimensional Ising behavior that is crossed, or no such regime at all. Then a crossover from mean-field type behavior—very far from T_c—to two-dimensional Ising behavior occurs.

Unfortunately, the data for $\hat{B}_{\text{eff}}$ (Table II) are not accurate enough to allow any convincing check of Eq. (26): since the scaling prediction for the shift of T_c is seen for $D \geqslant 20$, only data for $D \geqslant 20$ are expected to be useful for checking Eq. (26) as well. Within our accuracy, $\hat{B}_{\text{eff}}(D)$ is constant for $D \geqslant 16$, and thus the decrease predicted in Eq. (26) is not observed. However, one must distinguish the true critical amplitude $\hat{B}(D)$—applying in the region very close to $T_c(D)$, where the true critical exponent $\beta_2 = 1/8$ determines the vanishing of the order parameter—from the effective amplitude $\hat{B}_{\text{eff}}$ in Table II, since for $D \geqslant 20$ the effective exponent β_{eff} deviates from β_2 distinctly.

Nevertheless these data are useful to discuss the phase diagram (Fig. 10). The expected flattening of the coexistence curve due to the crossover over to two-dimensional Ising behavior with decreasing film thickness is

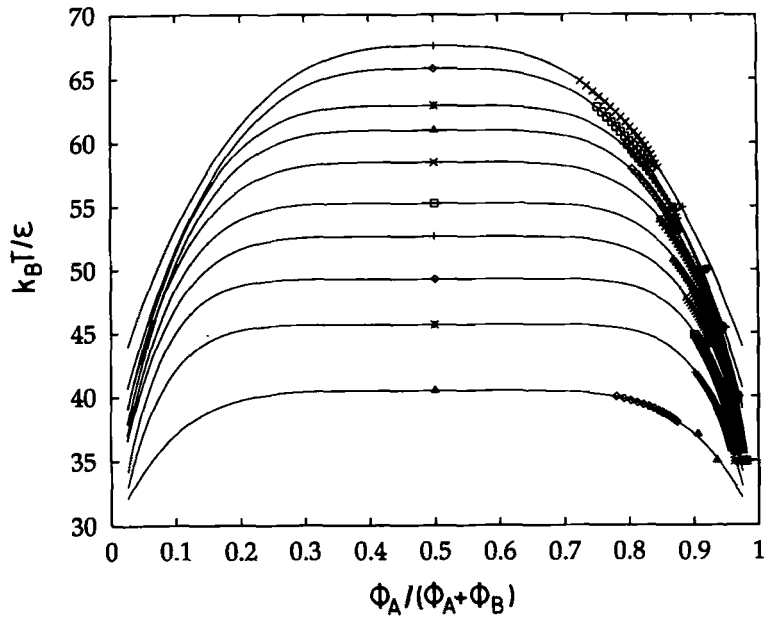

Fig. 10. Phase diagram T vs. $\phi_A/(\phi_A+\phi_B)$ of the unmixing transition in the thin film. The symbols refer to different film thicknesses: $D=8$, 10, 12, 14, 16, 20, 24, 28, 36, and 48 (from the bottom to the top). Note the strong flattening of the coexistence curve, particularly for thin films, which is not expected from Ginzburg–Landau theory (see text for details).

clearly seen. These coexistence curves are dramatically different from their (parabolic) mean-field counterparts (cf., e.g., Fig. 2 of ref. 15). Thus, if $T < T_c(D)$ one enters very quickly the strongly segregated regime of the polymer blend in the thin film.

Of course, in real systems one expects to encounter also deviations from the results discussed here due to the nonneutrality of the surfaces, i.e., the surfaces will typically preferentially attract one component of the blend. This effect leads to an additional distortion of the phase diagram: even if the phase diagram is symmetric in the bulk, it becomes asymmetric in the thin-film geometry.[13] This well-known consequence of "capillary condensation"[11–13] is expected to apply to polymer blends in thin-film geometry, too, but to our knowledge still needs to be explored in detail.

ACKNOWLEDGMENTS

One of us (Y. R.) is grateful to INRA and another (J. B.) to the Bundesministerium für Forschung und Technologie (BMFT; grant number

03M4076A3) for financial support of this work. Special thanks go to M. Müller for many helpful discussions during the various stages of this work and to S. Kumar for sending us preprints of refs. 15 and 16 prior to publication.

REFERENCES

1. S. Reich and Y. Cohen, *J. Polymer Sci., Polymer Phys. Ed.* **19**:1255 (1981).
2. A. Budkowski, U. Steiner, and J. Klein, *J. Chem. Phys.* **97**:5229 (1992).
3. U. Steiner, E. Eiser, J. Klein, A. Budowski, and L. J. Fetters, *Science* **258**:1126 (1992).
4. U. Steiner, J. Klein and L. J. Fetters, *Phys. Rev. Lett.* 72:1498 (1994).
5. F. Bruder and R. Brenn, *Phys. Rev. Lett.* **69**:1326 (1992); *Europhys. Lett.* **22**:707 (1993).
6. R. A. L. Jones, L. J. Norton, E. J. Kramer, F. S. Bates, and P. Wiltzius, *Phys. Rev. Lett.* **66**:1326 (1991); P. Wiltzius and A. Cumming, *Phys. Rev. Lett.* **66**:3000 (1991).
7. G. Krasuch, C.-A. Dai, E. J. Kramer, J. F. Marko, and F. S. Bates, *Macromolecules* **26**:5566 (1993).
8. K. Binder, in *Phase Transitions and Critical Phenomena*, Vol. 8, by C. Domb and J. L. Lebowitz, eds. (Academic Press, New York, 1983).
9. M. N. Barber, in *Phase Transitions and Critical Phenomena*, Vol. 8, C. Domb and J. L. Lebowitz, eds. (Academic Press, New York, 1983).
10. K. Binder, *Thin Solid Films* **20**:367 (1974).
11. M. E. Fisher and H. Nakanishi, *J. Chem. Phys.* **75**:5857 (1981); H. Nakanishi and M. E. Fisher, *J. Chem. Phys.* **78**:3279 (1983).
12. J. R. Evans, in *Fundamentals of Inhomogeneous Fluids*, D. Henderson, ed. (Dekker, New York, 1992); R. Evans, *J. Phys. C* **2**:8989 (1990).
13. K. Binder and D. P. Landau, *J. Chem. Phys.* **96**:1444 (1992).
14. K. Binder, *Annu. Rev. Phys. Chem.* **43**:133 (1992).
15. H. Tang, I. Szleifer, and S. K. Kumar, *J. Chem. Phys.* **100**:5367 (1994).
16. S. K. Kumar, H. Tang, and I. Szleifer, *Mol. Phys.*, in press.
17. E. Raphael, *J. Phys.* (Paris), in press.
18. H. P. Deutsch and K. Binder, *J. Phys.* II (Paris) **3**:1049 (1993).
19. H.-P. Deutsch and K. Binder, *Macromolecules* **25**:6214 (1992); H.-P Deutsch, *J. Stat. Phys.* **67**:1039 (1992).
20. M. E. Fisher, in *Critical Phenomena*, M. S. Green, ed. (Academic Press, London, 1971).
21. P. G. de Gennes, *J. Phys. Lett.* (Paris) **38**:L441 (1977).
22. K. Binder, *Phys. Rev. A* **29**:341 (1984).
23. H E. Stanley, *An Introduction to Phase Transitions and Critical Phenomena* (Oxford University Press, Oxford, 1971).
24. P. J. Flory, *Principles of Polymer Chemistry* (Cornell University Press, Ithaca, New York, 1953).
25. P. J. Flory, *J. Chem. Phys.* **9**:660 (1941); M. L. Huggins, *J. Chem. Phys.* **9**:440 (1941).
26. K. Binder, *Adv. Polymer Sci.* **112**:181 (1994).
27. M. E. Fisher, *Rev. Mod. Phys.* **46**:597 (1974).
28. J. C. Guillou and J. Zinn-Justin, *Phys. Rev. B* **21**:3976 (1980).
29. A. Sariban and K. Binder, *J. Chem. Phys.* **86**:5853 (1987); *Macromolecules* **21**:711 (1988).
30. G. Meier, D. Schwahn, K. Mortensen, and S. Janssen, *Europhys. Lett.* **22**:577 (1993); D. Schwahn, G. Meier, K. Mortensen, and S. Janssen, *J. Phys.* II (Paris) **4**:837 (1994).
31. K. Binder and J. S. Wang, *J. Stat. Phys.* **55**:87 (1989).

32. K. Binder, in *Finite Size Scaling and the Numerical Simulation of Statistical Systems*, V. Privman, ed. (World Scientific, Singapore, 1990).
33. W. Paul, K. Binder, D. W. Heermann, and K. Kremer, *J. Phys.* II (Paris) **1**:37 (1991).
34. I. Geroff, A. Milchev, W. Paul, and K. Binder, *J. Chem. Phys.* **98**:6526 (1993).
35. K. Kremer and K. Binder, *Comp. Phys. Rep.* **7**:259 (1988).
36. A. K. Kron, *Polymer Sci. USSR* **7**:1361 (1965); F. T. Wall and F. Mandel, *J. Chem. Phys.* **63**:4592 (1975).
37. M. Müller and K. Binder, *Comp. Phys. Commun.*, in press.
38. J. Baschnagel, K. Binder, W. Paul, M. Law, U. Suter, I. Batoulis, W. Jilge, and T. Bürger, *J. Chem. Phys.* **95**:6014 (1991); K. Binder, *Macromol. Symp.* **50**:1 (1991).
39. H.-P. Deutsch and K. Binder, *J. Chem. Phys.* **94**:2294 (1991).
40. J. S. Wang and K. Binder, *J. Chem. Phys.* **94**:8537 (1991).
41. I. Schmidt and K. Binder, *J. Phys.* (Paris) **46**:1631 (1985).
42. K. Binder and P. C. Hohenberg, *Phys. Rev. B* **6**:3461 (1972); **9**:2194 (1974).
43. D. P. Landau and K. Binder, *Phys. Rev. B* **41**:4633 (1990).
44. K. Binder, in *Computational Methods in Field Theory*, H. Graustere and C. B. Lang, eds. (Springer, Berlin, 1992).
45. F. Freirie, D. O'Connor, and C. R. Stephens, *J. Stat. Phys.* **74**:219 (1994).